Molecular relaxation dynamics in organic monolayer junctions

Stéphane Pleutin, Nicolas Clément, David Guérin, and Dominique Vuillaume
"Molecular Nanostructures and Devices" Group, Institute for Electronics, Microelectronics and Nanotechnology, CNRS and University of Sciences and Technologies of Lille, BP 690069, Avenue Poincaré, F-59652 Villeneuve d'Ascq, France
(Received 26 March 2010; revised manuscript received 25 June 2010; published 20 September 2010)

The complex admittance of various molecular junctions based on long alkyl chains (C18) has been measured and resolved into different components. The dipolar contribution of the response function has been analyzed in terms of the generalized Langevin equation. This formalism allows us to extract from experimental data the spectral density of polarization noise and to characterize the fluctuation dynamics of the molecules around their equilibrium positions. This spectral density is of $1/f$ type, characteristic of fractional Gaussian noise. It is suggested that the structural disorder of the junctions is at the origin of these polarization fluctuations. Possible relation between the $1/f$ tunnel current and polarization noises is also discussed.

DOI: 10.1103/PhysRevB.82.125436 PACS number(s): 77.22.Gm, 05.40.−a, 85.65.+h

I. INTRODUCTION

Self-assembled monolayers (SAMs) composed of hydrocarbon chains and small molecules are widely used nowadays. This is motivated by their relative ease of preparation and their chemical flexibility that allows controls at molecular level of the structure and chemistry of surfaces.[1] The range of applicability is large: they commonly serve as nanodielectric[2–5] and prototypes for molecular memories[6] or switches,[7–10] to name a few. In this context, to understand their electric properties is an important issue. However, most of the characterizations are done by dc electric measurements[11,12] or inelastic electron spectroscopies[13,14] that give limited information about the electric current (tunneling, resonant tunneling, etc.) and the molecular vibration modes excited by the current. More recently, electric noise in the low-frequency limit ($1/f$ noise) has been investigated giving additional information.[15] Increase in both electric current and electric noise for certain bias have been evidenced and explained by invoking interfacial traps and trap-assisted tunneling mechanisms associated to them.[15] In this work we discuss admittance spectroscopy which is a powerful technique to analyze relaxation mechanisms in a wide range of time scale. For many of the applications listed above it is essential to understand the response of the monolayer to ac signals.

The motion of single or ensemble of molecules are believed to influence significantly the thermal,[16] the mechanical,[17] and the transport properties[18] of the SAMs. They can be of large amplitude despite the close packing of the alkyl chains and the chemical links between the substrate and the molecules.[19,20] The low signal levels produced by SAMs coatings on planar surface prevent the application of standard techniques such as nuclear magnetic resonance that are conventionally used to detect such motions in materials.[16] However, admittance spectroscopy proves, in two recent works,[21,22] to be sensible enough to probe molecular relaxation associated to these motions. A first set of measurements have been performed on SAMs with varying coating densities and different substituent polar groups but using nanoporous substrates to scale up the surface area in order to increase the response signals.[21] The main drawback of this method is to consider complex geometry very different from what is commonly used in applications and that makes interpretation more difficult. In a second work, planar geometries have been considered with molecule densities varying from 10% of surface coverage to multilayer coverage. The excitation has been applied parallel to the surface of the substrate. The temperature has been varied but the range of frequencies centered about 1 kHz was very limited.[22]

We have done complex admittance measurements for usual planar geometry:[23] the alkyl chains are grafted on planar surfaces and contacted on top with metallic electrodes. A small ac signal (10 mV), with frequency ranging between 20 and 10^6 Hz, plus a dc bias varying from 0 to 1 V are applied perpendicular to the surface electrodes. The complex admittance shows three independent contributions due to tunnel current, interfacial defects, and molecular relaxation.[23] Here we focus on the theoretical analysis of the last contribution. As suggested also in Ref. 21, it is interpreted as due to small permanent dipoles present in the monolayer. With applied fields, these dipoles are displaced contributing to the polarization and dissipating energy by interactions with the environment. This dipolar contribution is shown to follow the universal behavior pointed out by Jonsher.[23,24] The imaginary part of the susceptibility vs frequency shows a peak with two power laws in the prepeak and postpeak regions. The exponents depend on the nature of the SAM and on the metallic electrodes (Al or Hg). In all cases the exponents and the peak position are very similar to the ones found in bulk amorphous organic polymers such as the polyethylene in the glass phase. However the dissipated energy is more important by one order of magnitude in our systems.

We analyze the data in terms of a Caldeira and Leggett type of model[25,26] that describes the dynamics of independent permanent dipoles trapped in harmonic potential and interacting with the harmonic modes of the SAMs (vibration, rotation) playing the role of a bath where the energy is dissipated. We choose this model for dissipation among several other possibilities[27] because, to our opinion, it is the simplest that fits our present understanding of the structure of the monolayer and mechanisms of dipolar polarization. Since the experiments are done at room temperature we neglect quantum fluctuations. This model is then equivalent to a classical generalized Langevin equation (GLE) where the friction

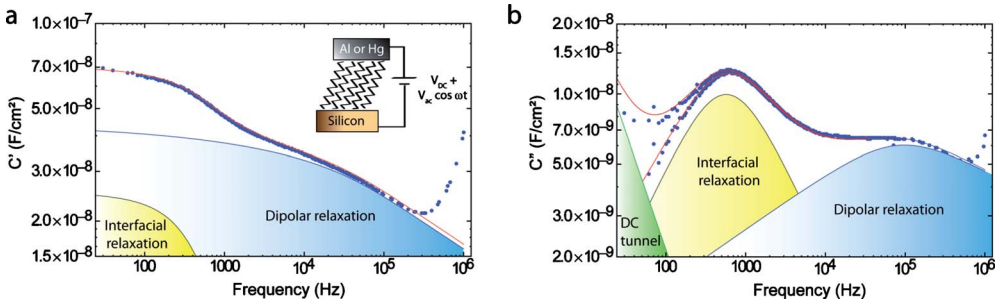

FIG. 1. (Color online) Typical complex admittance obtained for an OD junction with Al top electrode at $V_{dc}=0.1$ V, decomposed in (a) imaginary and (b) real parts. The experimental data (dots) are fitted (red lines) assuming three independent components (see text): a tunnel current contribution (filled in green), an interfacial contribution attributed to interface defects (filled in yellow), and a dipolar contribution attributed to the permanent dipoles of the monolayer (filled in blue). Note in the real part two sets of data: the top data corresponds to $\Re Y(\omega)/\omega$, the down data to $\Re Y(\omega)/\omega - G_T/\omega$ (see text). Inset of (a): schematic of the experiment.

term is non-Markovian.[28] In the framework of the GLE, the admittance spectroscopy is seen as a noise spectroscopy. A relation between the complex admittance that we measure and the spectral density of the bath fluctuations is naturally derived. These fluctuations entirely control the dynamics of the permanent dipoles participating to the polarization. In particular, it is shown that the dynamics of the dipoles is well described in terms of damped harmonic oscillator with fractional Gaussian noise.[29] This type of dynamics is rather widespread in nature being observed in very different systems; a recent appealing example concerns the distance separating the donor and acceptor sites of single protein complex.[30] From the power spectrum of the bath fluctuations we obtain the spectral density of dielectric—or polarization—noise. It is then suggested that the $1/f$ current noise observed in the very same systems[15] could be caused, at least partly, by the voltage fluctuation induced by the polarization noise. The generalized Langevin theory gives us a useful way to interpret our results and explain successfully part of our data such as the linear variation in the inverse of the characteristic time of relaxation of the permanent dipoles, $1/\tau$, with the applied dc voltage. However, to understand the physical mechanisms at the origin of the power laws observed in the complex admittance, more microscopic analysis of the mechanical properties of the SAMs are required. A first effort in this direction is proposed in this work relating the spectral density of polarization noise to the density of states of the harmonic modes of the SAMs.

The paper is organized as follows. In Sec. II some details about the devices and experiments are given. A model structure of our monolayer based on experimental observations is proposed in Sec. III; possible origins of the permanent dipoles are also discussed. Experimental data for the dipolar contribution of the susceptibility are shown and discussed in Sec. IV. In Sec. V the generalized Langevin equation used to interpret our data is presented and analyzed. The spectral densities of the fluctuations of the bath and of the polarization noise are obtained from the experimental susceptibility. Last a direct relation between the polarization noise and the $1/f$ current noise observed in a previous work[15] is suggested and discussed. In Sec. VI the effects of the dc field are included in our model and the variations in the characteristic time of relaxation are well reproduced. To conclude, qualitative arguments are developed in Sec. VII showing relation between the spectral density of the bath and the density of its harmonic modes (vibration and rotation of the SAM).

II. SAMPLES AND EXPERIMENTS

Two different types of monolayers were prepared, based on similar alkyl chains of 18 carbon atoms but with different terminal groups. The two alkyl monolayers are grafted on different silicon substrates following well-defined recipes described elsewhere.[31,32] In the first type, octadecyltrichlorosilane (OTS) molecules are grafted on 0.6-nm-thick oxide thermally grown on *n*-type doped (resistivity $\sim 10^{-3}$ Ω cm) Si(100).[31] In the second type, octadecene (OD) molecules are directly grafted on *n*-type doped (0.02–0.5 Ω cm) Si(111).[32] The quality of the monolayers was assessed by spectroscopic ellipsometry and water contact angle measurements. We selected only monolayers with a water contact angle larger than 110° and a thickness close (within 3 Å) to the theoretical expectation for a SAM with the molecules in their all-trans conformation. The monolayers were contacted by 50-nm-thick aluminum contact pads with different surface area between 9×10^{-4} cm^2 and 4×10^{-2} cm^2 or by a mercury drop. At the end, we have a set of similar molecular junctions that allows us to compare two types of silicon/molecule interfaces and two types of top metal contacts (see details in Ref. 23).

We have performed ac admittance spectroscopy.[23] All the measurements were done in dark, under controlled atmosphere (N_2) and at room temperature. A small ac signal (10 mV) superimposed to a dc voltage bias (0–1 V) was applied to the metallic electrodes, the Si was grounded and the complex admittance was measured using an impedance-meter Agilent 4284 A in the range 20–10^6 Hz [see inset of Fig. 1(a)]. Measured conductance and capacitance were corrected from small series resistances (typically in the range 5–70 Ω) according to a standard procedure.[33] There is still a small parasitic effect due to the sample environment (cables) that causes increase in the response at high frequencies. It is a known effect[34] but since it only affects the highest frequency part of the curves, we let it as it is (see Fig. 1). More details about the experimental procedure can be found elsewhere.[23]

The complex admittance $Y(\omega)$ can be expressed in terms of the tunnel conductance, G_T, and the macroscopic dielectric susceptibility, $\chi_M(\omega)=\chi'_M(\omega)+j\chi''_M(\omega)$, which is the response of the whole system to oppose to the local susceptibility which is the response of an individual dipole (Secs. IV and V). The tunnel conductance is assumed frequency independent. The real part of the susceptibility describes polarization phenomena while its imaginary part takes account for dissipation. We plot

$$\Re Y(\omega)/\omega = G_T/\omega + \frac{A\epsilon_0}{d}\chi''_M(\omega) = G_T/\omega + C''(\omega),$$

$$\Im Y(\omega)/\omega - C_\infty = \frac{A\epsilon_0}{d}\chi'_M(\omega) = C'(\omega), \quad (1)$$

where A is the surface area of the junction, ϵ_0 the permittivity of the vacuum, and d the interelectrode spacing. We have approximately $d_{\mathrm{OTS}}=2.5$ nm and $d_{\mathrm{OD}}=2$ nm (ellipsometry measurements). In the frequency range that we consider we probe the slow polarization mechanisms caused by permanent dipoles. C_∞ is the part of the capacitance due to ionic and electronic contribution. More precisely, it is defined for intermediate frequencies large enough for the dipoles to be frozen and not contributing to the polarization but small enough to not consider dissipation from the ionic and electronic degrees of freedom. $C(\omega)=C'(\omega)+jC''(\omega)$ is the part of the capacitance due to permanent dipoles.

Typical results are given in Fig. 1 for an OD junction with Al electrode at $V_{\mathrm{dc}}=0.1$ V. All the results that we have obtained—with different junctions and different dc potential—are qualitatively similar to this example.[23] The admittance shows three contributions that can be well identified in the real component—Fig. 1(b): a G_T/ω contribution due to tunnel current (filled in green) and two peaks at low frequencies (filled in yellow) and higher frequencies (filled in blue). The peaks correspond in the imaginary part of the admittance to plateaulike contributions [Fig. 1(a)]. The low-frequency peak is attributed to interfacial defects. Its amplitude strongly varies from device to device and these variations are related to changes by orders of magnitude in the dc conductance.[23] On the opposite the precise shape of the second peak at higher frequency depends only on the nature of the junction, OD or OTS, and of the top electrode, Al or Hg, but is very reproducible from device to device of the same set.[23] In particular, it is not affected by the amplitudes of the first peak and of the tunnel current. This contribution is interpreted as being the intrinsic susceptibility of the junction. In fact, the susceptibility contains two parts (interfacial and dipolar) and we write

$$\chi_M(\omega) = \chi_{int}(\omega) + \chi_{dip}(\omega). \quad (2)$$

The two parts are assumed to be independent as confirmed by experimental observations.[23] The interface part gives rise to the low-frequency peak and is due to some defects as briefly discussed above and that we have found to be located near the Si interface.[23] In this work we focus on the dipolar—or molecular—part of the relaxation.

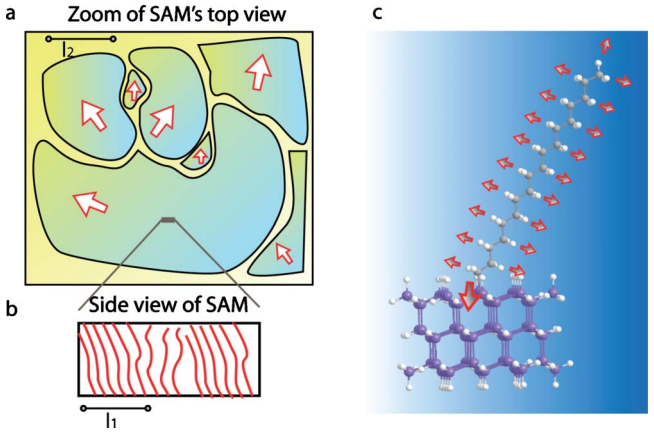

FIG. 2. (Color online) (a) Schematic top view of the monolayer. Each molecule is represented by a vector joining its two ends. The arrows are the projection of those vectors to the surface of the substrate. The monolayer appears as a collection of clusters, with characteristic size l_2 (~ 1 μm), defined by a certain direction separated from each other by grain boundaries. (b) Zoom of a cut in a particular cluster. The translational order appears to be very short with correlation length l_1 (~ 50 nm). (c) The two molecules studied in this work show weak permanent dipoles (~ 0.1 D) perpendicular to their backbone and two stronger dipoles at both ends (~ 1 D) more or less parallel to their axes. They both show a tilt angle [15° (30°) for OTS (OD)] with respect to the normal at the interfaces. The permanent dipoles are estimated (MOPAC software) using a model structure with small clusters of Si atoms.

At the frequencies considered in this work (≤ 1 MHz), we probe the relaxation mechanisms of permanent dipoles present in our system. Studies of the response should provide us information concerning the permanent dipoles themselves (amplitude, density) but also on structural aspects of their surrounding where the relaxation takes place. This is a crucial point. For instance, it is well known that the relaxation of permanent dipoles is considerably slowed down in glassy systems because of their amorphous structures.[35] First questions concern those two aspects. Where are the permanent dipoles located in our molecules? What is their magnitude? What is the kind of typical structure expected for the SAMs? Are they crystals or amorphous systems? In the next section structure models are proposed based on experimental evidences.

III. ORIGIN OF THE PERMANENT DIPOLES AND STRUCTURE OF THE SAMs

The two types of monolayers that we have investigated in this work are based on saturated molecules with 18 carbon atoms. These molecules are known to be weakly polar. Each CH bond perpendicular to the backbone of the molecules carries a small dipole of about 0.1 D. Such dipoles, even if they are weak are probably at the origin of the β relaxation observed for saturated polymers in amorphous phases.[35] In addition, in our systems, two stronger residual permanent dipoles are located at both ends of the molecules [see Fig. 2(c)]. One of these dipoles—the strongest—is induced by the substrate and is carried by the chemical bonds with the mol-

ecules [see Fig. 2(c)]. The magnitudes of those two local permanent dipoles may be roughly estimated by semiempirical calculations between 0.5 and 1 D (MOPAC software). In these simulations we have included clusters of Si atoms to accurately model the interfacial dipoles [see Fig. 2(c)]. Note that all these values are certainly overestimated since the Coulomb interaction between dipoles and with the metallic surrounding have not been included in the calculations. Strong dipolar effects cannot be expected here. However, we see in these interfacial dipoles, all more or less aligned in the same direction, a possible origin for the difference in amplitude of the peak of maximum loss observed in our systems and in bulk polymers.[35]

van der Waals interaction force the molecules to be packed together and aligned in the same direction at a tilt angle, θ, with respect to the normal to the substrate.[1] We estimate $\theta_{\mathrm{OTS}} \approx 15°$ and $\theta_{\mathrm{OD}} \approx 30°$ from ellipsometry measurements. In both cases the molecules are organized in a triangular lattice[1] with a nearest-neighbor distance of about 4.8 Å for OTS and slightly more, 5.1 Å, for OD.[36] The SAMs could, in principle, form well-ordered phases. However because of rotational invariance there is no preferred plan for tilting. During the formation of a monolayer, clusters grow up simultaneously from different positions on the substrate, having each a particular orientation. As a consequence the SAMs form polycrystals at the micrometer scale [l_2 in Fig. 2(a)], where organized clusters with a particular molecular orientation are separated by grain boundaries. This large-scale structure is expected for all types of SAM and was clearly observed for OTS and alkanethiols monolayers by atomic force microscopy.[37] The organization inside the clusters has been investigated by x-ray grazing diffraction incidence[38] and specular reflections[39] for OTS and other SAMs. Because of similarities between the different SAMs it is reasonable to expect the same qualitative characteristics for OD systems. The molecules appear to be packed with a volume per molecule of about 20 $\mathrm{Å}^2$ for OTS (and slightly more for OD, approximately 25 $\mathrm{Å}^2$) but with a very short in plane correlation length of 45 Å [l_1 in Fig. 2(b)]. This suggests a liquidlike organization within the plane. A schematic side view inspired by Ref. 39 is shown in Fig. 2(b). In addition, a thin electrode is in our case deposited on top of the monolayer: the SAM is sandwiched between the substrate and the top electrode. The molecules are therefore strongly constraint due to the large packing density within the monolayer and the electrodes to which they are linked either chemically or physically. As a consequence they can react only weakly to an electric field.

Because of their peculiar structural organization we expect the dielectric response of the SAMs to be nonuniform: most of the molecules may be quasi-inactive under the action of an external electric field while some of them—or at least segments of some molecules—may have more space to move and, as a consequence, may be more flexible. These "mobile" molecules are likely to be located at the grain boundaries or at some other structural defects inside the clusters where the molecule density is reduced and the constraints are somehow relaxed (see Fig. 2). The local permanent dipoles of those molecules are then mobile, or partially mobile, and are consequently able to follow more easily the applied electric field: in this picture only part of the SAM contributes significantly to the total dipolar polarization. The average induced displacement of the permanent dipoles, of amplitude $\delta\mu$, determines the magnitude of the dipole contribution to the capacitance. It should depend on the chain density and on the nature of the electrodes. The OTS samples are denser than the OD samples. We expect therefore $\delta\mu$ to be more intense for OD. We can estimate this quantity from the low-frequency capacitance. After subtracting C_∞ and the part due to the interface traps we are left with a pure dipolar contribution C_{dip}. We write using the same kind of qualitative arguments developed in Ref. 40,

$$\tilde{C}_{dip} = \frac{\delta\mu}{AdV_{\mathrm{dc}}}, \tag{3}$$

where d is the SAM thickness and V_{dc} is small (in practice we have taken $V_{\mathrm{dc}}=0.1$ V). $\tilde{C}_{dip}$ is the dipolar capacitance per unit surface; we have from typical experimental values 3×10^{-8} F cm^{-2} and 4×10^{-8} F cm^{-2},[23] for OTS and OD, respectively. From the volume per molecule estimated by x-ray experiments there is approximately 5×10^{13} molecules of OTS and approximately 1.25 time less of OD, for a sample with a surface $A=10^{-2}$ cm^2. From these values we extract $\delta\tilde{\mu}=\delta\mu$/molecule. We find 4.5×10^{-3} D and 6×10^{-3} D for OTS- and OD-based junctions, respectively. This difference may reflect the different molecular density of the molecular junctions, as stressed above. The amplitude of the peak of maximum loss should depend on the magnitude of the relaxing dipoles and of their faculty to fluctuate around their equilibrium position. The amplitude of these fluctuations should be related to the density of molecules of the SAMs. Indeed, the loss peak is more pronounced for OD than OTS type of junctions.[23]

When the dipoles are reoriented by the applied field they affect also the rest of the monolayer due to the interaction that exist between molecules. The reorientation of the dipoles and the disturbance that these motions induce in the surrounding of the dipoles are both responsible for the observed dielectric susceptibility.

IV. ELECTRIC SUSCEPTIBILITY AND RELAXATION FUNCTION—DEBYE VS UNIVERSAL BEHAVIOR

The dipoles are considered as independent or, in other words, their mutual interaction is assumed to be taken in a mean-field manner. We focus now on a single dipole and hence to the local susceptibility, χ, associated to it. The macroscopic susceptibility of Eq. (1), χ_M, is simply proportional to χ as will be seen in more details in Sec. V. Moreover, as already stressed in Sec. II, we consider throughout this work that the dipolar contribution can be treated independently of the tunnel current and of the interfacial part of the admittance. This assumption seems in agreements with our experimental observations.[23]

In linear-response theory (weak ac field), the complex dielectric susceptibility is related to the relaxation function, φ, which is the response function of the system after the abrupt removal of a constant electric field at $t=0$.[41] In our case, the

relaxation function describes the way the dipoles relax toward a stable equilibrium once the perturbation has been removed,

$$\chi(\omega) = \chi'(\omega) + j\chi''(\omega) = (\chi_0 - \chi_\infty)\left[1 + j\omega\int_0^{+\infty} dt\varphi(t)e^{j\omega t}\right], \tag{4}$$

where χ_0 is the value at zero frequency. We take $\chi_\infty=0$, meaning that at high enough frequencies the dipole cannot follow the field anymore and do not contribute to the polarization. Equation (4) is well defined in the context of equilibrium statistical mechanics: this is the fluctuation dissipation theorem (FDT).[41] We observe anomalous relaxation following power laws, as it will be clear below, that make transient dynamics very slow. This type of relaxation is known to add complication to Eq. (4).[42,43] However it was shown in Ref. 26 that the FDT is recovered by adding an additional averaging over the initial condition of the relaxation. We will come back to this point in Sec. V with a little more details and the proper definition of the relaxation function φ.

In the simplest case, considered long ago by Debye, the relaxation function is given by a single exponential[44]

$$\varphi_{Debye}(t) = e^{-t/\tau}. \tag{5}$$

τ is the characteristic time of relaxation. The exponential law may be obtained by using a variety of microscopic models for relaxation process. This equation was first derived by Debye by considering the rotational Brownian motion (excluding the inertial effects) of an assembly of noninteracting dipoles.[44] His treatment is appropriate for a dilute solution of polar molecules with axial symmetry in an isotropic and nonpolar liquid. Such simple response yields[44]

$$\chi_{Debye}(\omega) = \chi_0\frac{1 + j\omega\tau}{1 + \omega^2\tau^2}. \tag{6}$$

The real part of Debye's susceptibility shows a plateau at low frequencies below $1/\tau$ and decreases as ω^{-2} above $1/\tau$. Its imaginary part shows a peak at $1/\tau$: it increases as ω in the prepeak region and decreases as ω^{-1} in the postpeak region. However, this type of response is hardly seen in condensed matter. Instead, fractional power laws are most often observed[24]

$$\chi(\omega) \propto (j\omega)^{n-1} \quad \text{for} \quad \omega \gg \omega_P,$$

$$\chi_0 - \chi(\omega) \propto (j\omega)^m \quad \text{for} \quad \omega \ll \omega_P. \tag{7}$$

ω_p being the frequency of maximum loss which is equal to $1/\tau$ in the Debye case but is a function of τ and of the two exponents, n and m, for more general cases. This is the famous "universal" dielectric response pointed out by Jonscher[24] but observed long before by many authors in very different systems (amorphous systems, van der Waals crystals, ionic solids, etc.). Several phenomenological expressions have been proposed over the years to mimic this behavior such as the Cole-Cole,[45] Cole-Davidson,[46] or Havriliak-Negami[47] (HN) dielectric susceptibilities. A suitable expression that models remarkably well our data is the Dissado-Hill[48] (DH) dielectric susceptibility. It reads

$$\chi_{DH}(\omega) = \chi_0\frac{\Gamma(1+m-n)}{\Gamma(m)\Gamma(2-n)}(1 - j\omega\tau)^{n-1}{}_2F_1[1-n, 1-m; 2-n; (1-j\omega\tau)^{-1}], \tag{8}$$

where ${}_2F_1$ is the Gauss hypergeometric function,[49] $0 \le m \le 1$ and $0 \le n \le 1$. Dissado and Hill have proposed this function based on some handling arguments. The details of their derivation are difficult to follow and some of their assumptions seem even hard to justify.[48] Nevertheless their function has proven to model successfully numerous data of very different systems. As the HN model, the DH function shows asymptotic fractional power laws both in the prepeak and postpeak region [Eq. (7)]. However, the two models differ noticeably in a frequency interval around the peak that can be a few decades large.[50] The particular shape of the HN function is not appropriate to our cases (see Figs. 4 and 6 of Ref. 50). The DH expression gives much better agreements with our data.

TABLE I. Parameters of the Dissado-Hill susceptibility obtained by fitting our data and averaging over six or eight samples depending on cases. Three cases are considered: OD junctions at $V_{dc}=0.1$ V and $V_{dc}=1$ V, and OTS junction at $V_{dc}=0.1$ V. The top electrode in these three cases is made of Al.

	OD (0.1 V)	OD (1 V)	OTS (0.1 V)
m	0.22	0.1	0.13
n	0.8	0.85	0.85
$1/\tau$ (kHz)	150	330	370

To match our data, together with a tunnel contribution a linear combination of two DH dielectric susceptibilities has been considered (see Fig. 1). This point was already discussed in Sec. II [see Eqs. (1) and (2)]. If we omit the high frequency, increases known to be a parasitic effect caused by the environment of the junction,[23,34] our fitting procedure gives good agreements with our data (see Fig. 1). It turns out that the interface part is well fitted by considering $n=0$ and $m=1$, which corresponds to a Debye type of response. The dipole part follows the universal behavior of Jonscher.[24] Table I gives experimental results for the dipolar part. We choose to quote the values of n, m, and τ for OD systems at 0.1 and 1 V (dc voltage) and for OTS systems at 0.1 V. The parameter values are obtained after averaging over six or eight samples depending on cases. Note that the observed dispersions for each parameter are rather small. This set of values is representative and sufficient to point out some important information. (i) The parameters of relaxation depend on the nature of the molecules in the SAM, OD, or OTS. (ii) The parameter values change by applying a dc electric field perpendicular to the surface electrodes. Interestingly, we can notice that the parameter values for OD with constant electric field (at 1 V) are close to the ones of OTS almost without field (at 0.1 V). Changes in the DH parameters with the nature of the electrodes is also observed and commented elsewhere.[23] Note that with the parameters of Table I, the

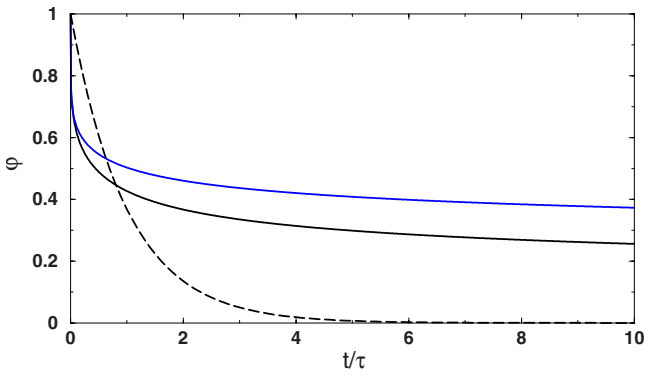

FIG. 3. (Color online) Relaxation functions related to the Debye (dashed line) and to the DH (full line)—with $n=0.85$ and $m=0.2$ (the down curve in black), and $n=0.85$ and $m=0.1$ (the top curve in blue)—susceptibilities.

asymptotic behaviors of the DH susceptibility are very close to the ones of the Cole-Cole model,[45] $\chi_{Cole\text{-}Cole}(\omega) \propto (j\omega)^{\alpha}$, for $\omega \ll \omega_P$, and $\chi_{Cole\text{-}Cole}(\omega) \propto (j\omega)^{-\alpha}$, for $\omega \gg \omega_P$, with $\alpha = n-1$: in our case, we obtain $\alpha \simeq 0.2$ for OD at 0.1 V and $\alpha \simeq 0.1$ for OD at 1 V and OTS at 0.1 V. As a final remark on this table we may notice that all the values reported here are typical for imperfectly crystallized materials such as glasses or vitreous polymer systems.[35] Typical examples concern nonpolar polymers such as poly-γ-benzyl-L-glutamate on NaCl plates,[48] epoxy resin at temperatures below the glass transition[51] and perhaps, the most interesting for us, the polyethylene—the polymer counterpart of our molecules—in the glass phase.[35] All of these examples show DH parameters very similar to those measured for our SAMs. X-ray diffraction studies on OTS (Refs. 38 and 39) favor the analogy between our systems and the nonpolar polymers cited above which show very poor translational order.

The relaxation function corresponding to the DH susceptibility can be derived from Eq. (4). One gets

$$\varphi_{\mathrm{DH}}(t) = 1 - \frac{\Gamma(1+m-n)}{\Gamma(2-n)^2\Gamma(m)}(t/\tau)^{1-n}{}_2F_2(1-n,1+m-n;2-n,2-n;-t/\tau), \tag{9}$$

where ${}_2F_2$ is a hypergeometric function.[49] In Fig. 3, as a matter of illustration, φ_{Debye} and φ_{DH} are shown in units of τ for typical parameters ($n=0.85$, $m=0.2$) and ($n=0.85$, $m=0.1$). One can notice that the dynamics of relaxation in our systems is dramatically slowed down compared to Debye's relaxation as usually observed for glassy systems. φ_{DH} reduces asymptotically (at short, $t<\tau$, and large, $t>\tau$, time) to power laws. This is typical of fractional Brownian motion.[26,29,30] The slowing down of the relaxation is usually understood as the result of interaction between the relaxing quantities—here the permanent dipoles—and low-energy excitations present in the system. This type of complex relaxation is described in terms of system plus reservoir models such as the one due to Caldeira and Leggett.[25,28] In the next section such model is used to establish a relation between the measured dielectric susceptibility and the spectral density of polarization noise. The reader not interested by technical details may switch directly to Eq. (24) relating the spectral density of the fluctuating bath to the measured complex susceptibility.

V. GENERALIZED LANGEVIN EQUATION—NOISE CHARACTERISTICS

Following closely Ref. 26, we consider a monolayer as an ensemble of dipoles μ_i with disordered orientation ϕ_i^0, that can be dynamically reoriented $\phi_i(t)=\phi_i^0+\delta\phi_i(t)$. These are the mobile dipoles of Sec. III. They are trapped in a potential assumed to be harmonic, $H_{trap}=k_i\delta\phi_i(t)^2/2$, and interact with the electric field, the dc and ac components; we first consider only the ac component $E_{\mathrm{ac}}(t)=E_{\mathrm{ac}}\cos(\omega t)$. The interaction between the dipoles and the applied field reads, as usual, $H_{int}=\mu_i\cos\phi_i(t)E_{\mathrm{ac}}(t)$ that yields after an expansion in $\delta\phi_i(t)$,

$$H_{int} = \mu\cos\phi(t)E_{\mathrm{ac}}(t) \approx \mu_{\parallel}E_{\mathrm{ac}}(t) - \mu_{\perp}\delta\phi(t)E_{\mathrm{ac}}(t). \tag{10}$$

We note $\mu_{\parallel}=\mu\cos\phi^0$ and $\mu_{\perp}=\mu\sin\phi^0$ the components of the dipole parallel and perpendicular to the electric field, respectively. In this expression and in the following we omit the indices for convenience. The mobile dipoles are subjected to friction as a consequence of their interaction with the environment that can be modeled in several ways.[25,27,28,52] To be consistent with our present understanding of the molecular junctions,[15,23] a satisfying and rather general model of the environment should include the harmonic modes of the monolayer (vibration and rotation modes) and a set of two-level systems that model defects such as the ones considered to analyze the $1/f$ current noise[15] or the interfacial peak of Fig. 1.[23] These are the so-called harmonic oscillator[25] and spin baths,[52] respectively. They are known to give different behaviors.[53] In particular, the part of the dissipated energy from the oscillating mobile dipoles to a spin bath decreases strongly at high temperatures on the contrary to the part given to the harmonic oscillator bath that increases. Since the experiments are done at room temperature, we expect the effects of a spin bath to be weak. Therefore, as a first step, we consider in this work oscillator bath only. It has to be understood that the consequences of this approximation should be tested in future works, by varying the temperature for instance.

The mobile dipoles interact with an infinite number of harmonic modes (bath). These harmonic modes can be, for instance, the rotation or vibration modes of the monolayer. We neglect explicit dipole-dipole interaction terms. The total Hamiltonian is then written as

$$H = \frac{J\delta\dot{\phi}(t)^2 + k\delta\phi(t)^2}{2} - \mu_{\perp}\delta\phi(t)E_{\mathrm{ac}}(t) + \frac{1}{2}\sum_{\alpha=1}^{N} J_{\alpha}\delta\dot{\phi}_{\alpha}(t)^2 + k_{\alpha}\left[\delta\phi_{\alpha}(t) - \frac{c_{\alpha}}{k_{\alpha}}\delta\phi(t)\right]^2, \tag{11}$$

where J is the inertial moment of the dipole. The first term of H_{int} has been dropped out since it does not contribute to the dynamics of the dipole. The last term of this Hamiltonian

models the harmonic bath (N modes, N assumes to be "infinite") that interacts linearly with the dipole. J_α and k_α are the inertial moment and the elastic constant of the mode α, c_α is the coupling between the mode and the dipole. This is a Caldeira-Leggett type of Hamiltonian introduced to study quantum dissipation.[25,28] The central ingredient in such model is the product of the density of modes of the bath times the squared coupling strength; this is the so-called spectral density of the environmental coupling[28]

$$\gamma(\omega) = \sum_{\alpha=1}^{N} \frac{c_\alpha^2}{J_\alpha \omega_\alpha} \delta(\omega - \omega_\alpha) \tag{12}$$

with $\omega_\alpha = \sqrt{k_\alpha / J_\alpha}$. If the noise (the bath) is characterized the dynamics of the system is fully determined. The spectral density γ could be, in principle, derived from detailed microscopic calculations. In practice, it is more often taken as a phenomenological function to be determined by experiments. This is the strategy followed in this work. Our objective is to determine this quantity giving the experimental susceptibility $\chi_{dip}(\omega) \propto \chi_{\mathrm{DH}}(\omega)$. In this approach the admittance spectroscopy can be seen as a kind of fluctuation spectroscopy.

In the following, we neglect quantum fluctuations (high-temperature limit). From Hamiltonian (11) the equations of motion for $\delta\phi$ and $\delta\phi_\alpha$ can be readily written down and, after elimination of the bath variables, the dipole coordinates are shown to follow the generalized Langevin equation (GLE),[28]

$$J\delta\ddot{\phi} + \int_0^t \eta(t-t')\,\delta\dot{\phi}(t')dt' + k\,\delta\phi(t) = \xi(t) + \mu_\perp E_{\mathrm{ac}}(t), \tag{13}$$

where

$$\eta(t) = \sum_\alpha \frac{c_\alpha^2}{J_\alpha \omega_\alpha^2} \cos\,\omega_\alpha t = \int_0^{+\infty} d\omega \frac{\gamma(\omega)}{\omega} \cos\,\omega t \tag{14}$$

and $\xi(t)$ is a Gaussian random field related to the damping kernel—or memory-friction kernel $-\eta(t-t')$ by the fluctuation-dissipation theorem,

$$\langle \xi(t)\xi(t') \rangle = k_B T \eta(t-t'). \tag{15}$$

$\langle\ \rangle$ represents the mean over thermal noise. The average is taken by considering the system bath plus dipole frozen at coordinates $\delta\phi(0)$ and $\delta\dot{\phi}(0)$ in thermal equilibrium.[28] T is the equilibrium temperature of the bath. In this new formulation, the memory kernel is the central quantity. We note $\eta(t) = \eta_S f(t)$, η_S being the friction coefficient (Stoke coefficient) and $f(t)$ a function without dimension. η_S is related to the bath parameters [Eq. (14)].

We can derive from the GLE [Eq. (13)], an equation for the relaxation function [see Eq. (4)] defined as a time correlation function at zero field,

$$\varphi(t) = \overline{\langle \delta\phi(t)\,\delta\phi(0) \rangle}. \tag{16}$$

The symbol $\bar{O}$ (O a function) means that an additional averaging over the initial fluctuation $\delta\phi(0)$ has been performed. By multiplying each term of Eq. (13) by $\delta\phi(0)$ and doing the different averages considering $\overline{\delta\phi(0)} = 0$, we get

$$J\ddot{\varphi} + \int_0^t \eta(t-t')\dot{\varphi}(t')dt' + k\varphi(t) = 0. \tag{17}$$

This procedure corresponds to our macroscopic experiment where we probe not a single mobile dipole but a huge assembly of them each supposed to respond independently. From Eq. (17) we can derive the fluctuation dissipation theorem [Eq. (13)]. This theorem is valid only because we have performed the additional averaging procedure.[26,43]

The dipole dynamics is assumed to be highly overdamped ($J \to 0$) as in the first model of Debye.[44] The Langevin equation [Eq. (13)] is then solved by Laplace's transform.[26] $\tilde{O}$ denotes the Laplace transform of O,[26,43]

$$\delta\tilde{\phi}(s) = \tilde{\eta}(s)\tilde{\chi}(s)\,\delta\phi(0) + \tilde{\chi}(s) \times \left(\tilde{\xi}(s) + \frac{1}{2}\mu_\perp E_{\mathrm{ac}} \left[\frac{1}{s - j\omega} + \frac{1}{s + j\omega} \right] \right) \tag{18}$$

with

$$\tilde{\chi}(s) = \frac{1}{k + s\tilde{\eta}(s)} \tag{19}$$

the Laplace transform of the dielectric susceptibility. The first term on the right-hand side of Eq. (18) gives the relaxation of the dipole starting from the initial fluctuation $\delta\phi(0)$. It also corresponds to the relaxation function of the system [Eq. (16)] obtained by solving directly Eq. (17) by Laplace transform,

$$\tilde{\varphi}(s) = \tilde{\eta}(s)\tilde{\chi}(s) = \frac{\tilde{\eta}(s)}{k + s\tilde{\eta}(s)}. \tag{20}$$

With the model, Eq. (13), we have $\chi_0 = 1/k$—meaning that the more the dipoles are constraint the less important is the dipolar contribution to the admittance—and $\tau = \eta_S / k$—meaning that the more the dipole is constraint the more rapidly it goes back to equilibrium and that the more the friction is important the more this way back is slowed down.

Before studying in more details the solution of the GLE it is necessary to connect the local and the macroscopic susceptibilities [Eq. (1)]. We assume the local and the macroscopic fields to be the same, for simplicity. This approximation should be reasonable since the organic monolayers are weakly polar. The Fourier transform of the average dipole displacement is obtained from Eq. (18) by performing averaging over the thermal noise and initial fluctuations,

$$\overline{\langle \delta\mu(\omega) \rangle} = \mu_\perp \overline{\langle \delta\phi(\omega) \rangle} = \mu_\perp^2 \chi(\omega) E_{\mathrm{ac}}(\omega). \tag{21}$$

From the last equation the macroscopic dipolar polarization vector by unit volume is obtained

$$P_{dip}(\omega) = M\overline{\langle \delta\mu(\omega) \rangle} = M\mu_\perp^2 \chi(\omega) E_{\mathrm{ac}}(\omega), \tag{22}$$

where M is the number of dipoles (or molecules) by unit volume. Writing, as usual, $P_{dip}(\omega) = \epsilon_0 \chi_{dip}(\omega) E(\omega)$ we get the expected simple relation

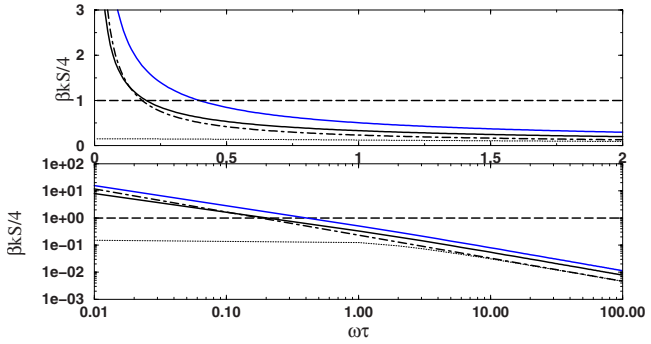

FIG. 4. (Color online) Spectral density (linear and log-log plot) of the dielectric noise [Eq. (24)] in units of k_BT/k related to the DH susceptibilities (full lines) with $n=0.85$ and $m=0.2$ (the down curve in black) and $n=0.85$ and $m=0.1$ (the top curve in blue), to the Debye susceptibility (dashed line) Ref. 44), to the Cole-Cole susceptibility (Ref. 45) with $n=0.85$ (dotted-dashed line), and to the Cole-Davidson susceptibility (Ref. 46) with $n=0.85$ (dotted line).

$$\chi_{dip}(\omega) = \frac{M\mu_\perp^2}{\epsilon_0}\chi(\omega). \tag{23}$$

This last relation establishes connection between solutions of the GLE and the experimental data.

Simple manipulations summarized in Appendix A, allow to relate the local dielectric susceptibility to the spectral density of the random field, $\xi(t)$,

$$S(\omega) = 4k_BT\frac{\Im\chi(\omega)}{\omega|\chi(\omega)|^2}. \tag{24}$$

In Fig. 4 (linear and log-log plot), we show two examples of spectral density derived from our data corresponding to the relaxation functions of Fig. 3. As a matter of illustration, the spectral densities of usual model susceptibilities given in Appendix B are also shown. These are models that produce simple analytical expressions to compare with. They reflect very different type of dynamics of the mobile dipoles. The Debye model[44] corresponds to usual Brownian motion,[54] the Cole-Cole model[45] to stochastic motion with fractional Gaussian noise.[30] The Cole-Davidson model[46] presents the two characteristics: it is Debye type at low frequencies and Cole-Cole type at high frequencies.

As can be seen in Fig. 4, at high enough frequencies the DH, and Cole-Davidson spectral densities are reduced to simple power laws as the Cole-Cole case. With the Havriliak-Negami susceptibility,[47] not explicitly considered here, we also obtain the same qualitative behaviors. Therefore, we expect similar noise properties at high frequencies ($\omega\tau \gg 1$) for all these different models, except Debye. Moreover, in our case, on the contrary to the Cole-Davidson case, we expect the same type of dynamics not only at high frequencies, but also at lower frequencies where the spectral density again tends to power laws but with slightly different exponents. To summarize, the spectral densities that we extract from our data of dielectric susceptibilities are qualitatively similar to the Cole-Cole model: we expect therefore the dipoles to follow a subdiffusion.[30] However, contrary to the Cole-Cole model the characteristics of the fluctuating

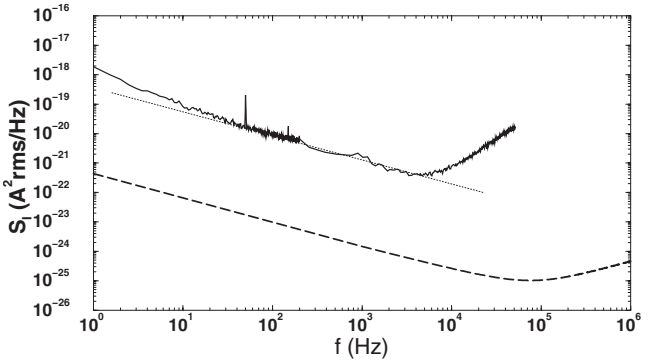

FIG. 5. Spectral density of tunnel current noise. The experimental data (full line) are obtained for an OD junction at $V_{dc}=0.8$ V. The power law is well reproduced by the theory (dashed line) but not the amplitude.

bath are changing with frequencies: they are always characteristics of a fractional Gaussian noise but with a value of the Hurst index that slightly depends on the frequency window considered.

The spectral density of the bath is simply related to the spectral density of polarization fluctuations, S_P. Indeed, starting from Eq. (18) without external field we get after averaging over the initial fluctuation the following simple relation between autocorrelation functions:

$$\overline{\langle \delta\tilde{\phi}(j\omega)\delta\tilde{\phi}(-j\omega)\rangle} = |\chi(\omega)|^2\overline{\langle \delta\tilde{\xi}(j\omega)\delta\tilde{\xi}(-j\omega)\rangle}. \tag{25}$$

From this last equation we can straightforwardly write

$$S_P(\omega) = \frac{M\mu_\perp^2}{\epsilon_0}|\chi(\omega)|^2 S(\omega) = \frac{M\mu_\perp^2}{\epsilon_0}\frac{\Im\chi(\omega)}{\omega} = \frac{\Im\chi_{dip}(\omega)}{\omega}. \tag{26}$$

Such spectral density gives a Lorentzian in the case of Debye and power laws for the other models. This is an important expression to be tested by future experiments. It synthesized all the approximation contained in our model [Eqs. (11), (13), and (23)]. This quantity cannot be measured directly but appears in the spectral density of voltage and current fluctuations as explained below.

The $1/f$ current noise of molecular junctions was already investigated in the frequency range from 0 to 100 Hz (see Fig. 5).[15] It shows two main characteristics. (i) The background noise power spectrum is proportional to $(\partial I/\partial V)^2$, I the tunnel current, V the applied voltage, suggesting pure capacitive effects. (ii) Strong local increase in noise appear at certain bias voltages. As usual, we have interpreted the data in terms of fluctuating defects modeled by independent two-level systems:[15,55] each defect is described by two possible states, the population of those states fluctuating with time. The first point was attributed to voltage fluctuations induced by the fluctuating two-level systems. The second point was explained by important changes in tunnel resistance at certain voltages induced by the modifications of the defect states through assisted tunneling mechanisms.[15] However, to our opinion this common interpretation suffers several drawbacks.[56] (i) The physical nature of the two-level systems

remains unknown. (ii) Arbitrary assumptions on the energy and time relaxation densities have to be done to get the expected $1/f$ behavior. (iii) More importantly, to reproduce the very large noise amplitude that we observed we are forced to consider unphysically large density of such defects: in some cases we obtain more defects than atoms present in the molecular dielectric. We have then to look for better interpretation with better physical grounds. For instance, is the $1/f$ polarization noise characterized in this work a possible candidate for the background noise observed in experiments?

In a dielectric, the voltage noise is due to the thermal fluctuations of the polarization.[57] In particular, there is no thermal motion of charge carriers as in any conductor. The Nyquist formula for the spectral density of voltage fluctuations, S_V, across a (macroscopic) capacitor gives[57]

$$S_V(\omega) = 4k_B T \frac{\Im C(\omega)}{\omega |C(\omega)|^2}. \tag{27}$$

Considering only the molecular fluctuations characterized in this work, we write

$$S_V(\omega) = \frac{4k_B T d}{A\epsilon_0} \frac{S_P(\omega)}{|[\epsilon_{r\infty} + \chi'_{dip}(\omega)]^2 + \chi''^2_{dip}(\omega)|}, \tag{28}$$

where $\epsilon_{r\infty}$ is the dielectric constant at high frequencies due to electrons (to be related to C_∞). This prediction may be tested by measuring the voltage fluctuation at zero dc field instead of the current fluctuations. This will be done in future work. Here we focus on the $1/f$ tunnel current noise to see if it is consistent with these voltage fluctuations. Note that in general there is also an interfacial contribution to this polarization which, however, could be considerably reduced by heating process.[23]

The polarization noise produces a fluctuating current—a polarization current—that shows an increasing spectral density with frequency[57]

$$S_I^P(\omega) = 4k_B T \omega \Im C(\omega). \tag{29}$$

This kind of noise is not explicitly observed in the frequency window considered in Ref. 15 (see Fig. 5) but could be seen at higher frequencies. This point needs to be further investigated. On the other hand the current flowing through the tunnel resistance is also fluctuating because of the fluctuating voltage. The experimental data suggest that these fluctuations are predominant in our systems at low frequencies.[15] Assuming a nonfluctuating tunnel resistance, the current fluctuations are simply related to voltage fluctuations,

$$\langle \delta I(t) \delta I(t') \rangle = \left(\frac{\partial I}{\partial V} \right)^2 \langle \delta V(t) \delta V(t') \rangle, \tag{30}$$

where $\delta O(t) = O(t) - \langle O \rangle$. The spectral density of current noise is then related to the spectral density of voltage noise,

$$S_I(\omega) = \left(\frac{\partial I}{\partial V} \right)^2 S_V(\omega). \tag{31}$$

With this expression, the spectral density of current shows a $(\partial I/\partial V)^2$ dependence as observed in experiment.

In Fig. 5, we compare the prediction of Eq. (31) with typical data (obtained at $V_{dc}=0.8$ V). The power law is well reproduced but not the amplitude: a factor of about 10^3 or 10^4 is missing in the theory. In this expression we consider only the voltage fluctuations caused by the permanent dipoles of the SAMs. Adding the interface [Eq. (2)] and the displacement current contributions [Eq. (29)] increases S_I but certainly not in a sufficient way. As a matter of illustration, the latter contribution is added to the spectral density in Fig. 5 and shown to contribute significantly to the total signal for frequencies higher than 10^5 Hz only. It seems therefore clear that the polarization noise alone cannot explain the large amplitude of the current noise. An important drawback of Eq. (31) concerns the assumption of constant tunnel resistance, consistent with the use of Eq. (27). Indeed, fluctuations of the dielectric properties, as the ones evidenced in this work, will induce fluctuations in the potential profile through the junction and, therefore, changes in the tunnel resistance. Additional investigations including both polarization and resistance noise induced by the same molecular fluctuations are needed to see whether the molecular fluctuations considered in this work are large enough, or not, to explain the unusual magnitude of the tunnel current noise. It is interesting to note that we have also seen effects of the low-frequency peaks in the tunnel current noise that perturb locally the $1/f$ law but in a way that cannot be simply explained by including the interfacial contribution in $S_V(\omega)$. This point is still under investigation and goes beyond the scope of the present work.

VI. EFFECTS OF THE dc ELECTRIC FIELD

In the experiments we apply a weak ac field plus a static potential varying from 0 to 1 V. Two main effects have been observed and summarized in Fig. 6. (i) The inverse of the characteristic time τ increases linearly with the dc field. (ii) The exponent m decreases. The first point is naturally explained with the GLE: this is the purpose of this section. The second point is beyond the scope of the effective theory used in this work.

The interaction of the dipole with the applied fields becomes

$$H_{int} = \mu \cos \phi(t) [E_{ac}(t) + E_{dc}]. \tag{32}$$

Expanding this expression yields

$$H_{int} \approx \mu_\parallel [E_{ac}(t) + E_{dc}] - \mu_\perp \delta\phi(t) [E_{ac}(t) + E_{dc}] - \frac{1}{2} \mu_\parallel [\delta\phi(t)]^2. \tag{33}$$

With this new interaction term, one can derive a generalized Langevin equation that is formally similar to Eq. (13) at the condition to consider shifted dynamical variables

$$\delta\phi \to \delta\phi + \frac{\mu_\perp}{k + \mu_\parallel E_{dc}} \tag{34}$$

and a new elastic constant

$$k \to k + \mu_\parallel E_{dc}. \tag{35}$$

These two transformations have clear meanings. (i) The center of mass of the harmonic oscillator is shifted by the con-

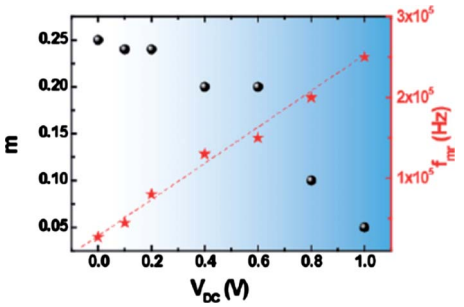

FIG. 6. (Color online) Typical evolution of m—one of the two exponents of the Dissado-Hill susceptibility (see text)—and $f_m = 1/\tau$ as function of $V_{\rm dc}$ for a particular OD junction.

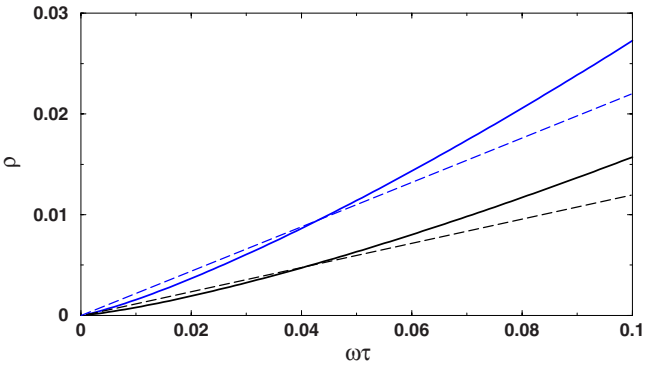

FIG. 7. (Color online) Density of harmonic modes related to the DH susceptibility with $n=0.85$, $m=0.2$ (the down curves in black) and $n=0.85$, $m=0.1$ (the top curves in blue), taking [see Eq. (37)]. The first case corresponds to the OD based devices without dc field, the second either to the OD with constant field [cf. Fig. 3(b)] or the OTS based devices without field. The two dashed curves are guide lines that serve to estimate the variations between the data and the linear densities expected for perfect monolayers.

stant field. (ii) The harmonic potential is strengthened by the dc potential, i.e., the constant field tends to align the mobile dipoles in its direction and therefore to reduce the angle fluctuations. The new Langevin equation is solved exactly as before. As a first consequence the inverse of τ is shifted up linearly by the constant electric field in agreements with experimental data,

$$\frac{1}{\tau} = \frac{k + \mu_{\parallel} E_{\rm dc}}{\eta_S}. \tag{36}$$

The dc potential perturbs also the harmonic modes of the environment in the same way it perturbs the dynamics of the dipoles. Since the dissipation is caused by the interaction between the permanent dipoles and the harmonic modes of the SAM, changes in the density of states should induce changes in the exponents of the Dissado-Hill susceptibility, Fig. 6.

VII. LOW-FREQUENCY VIBRATION MODES—QUALITATIVE ARGUMENTS

The energy dissipation is caused by the interaction of the dipoles with the harmonic modes of the bath, here the vibration and rotation modes of the monolayer. To get insight into the physical mechanisms at the origin of the particular response functions that we observe, a detailed knowledge both of these modes and of the way they interact with the permanent dipoles are needed. A full microscopic study of the mechanical properties of the monolayers is however a very complicated task. In this work we limit ourselves to a simple procedure assuming that $c_\alpha = \bar{c}$ and $J_\alpha = \bar{J}$ are α independent (these parameters remain constant for all harmonic modes). They can then be taken out of the summation in Eq. (14). The spectral density of environmental fluctuations is in this way simply related to the density of harmonic modes of our monolayer,

$$\rho(\omega) = \frac{1}{L^2} \sum_n \delta(\omega - \omega_n) \approx \frac{\bar{J}}{L^2 \bar{c}^2} \omega \gamma(\omega) = \frac{\bar{J}}{k_B T L^2 \bar{c}^2} \omega^2 S(\omega). \tag{37}$$

L being the characteristic size of the system. This crude approximation gives for the Debye susceptibility $\rho_{Debye}(\omega)$ $\propto \omega^2$ that corresponds to the density of independent three-dimensional isotropic harmonic oscillators, in agreements with the original statements of the Debye model.[44] For the more general susceptibility of Dissado and Hill, that corresponds to our observations, we get $\rho_{\rm DH}(\omega) \propto \omega^\sigma$ with σ depending on the frequency window considered but being always such that $1 < \sigma < 2$. In the case of the Cole-Cole model which should be strictly equivalent to ours for $\omega\tau > 1$ (see Fig. 4), $\sigma = 2 - n$ at all frequencies,

$$\rho_{Cole\text{-}Cole}(\omega) = \frac{4\bar{J}\tau^{1-n}}{L^2 \bar{c}^2 \chi_0} \omega^{2-n} \sin(1-n)\frac{\pi}{2}. \tag{38}$$

The densities of states, $\rho_{\rm DH}$, corresponding to the DH spectral densities of Fig. 4 are shown in Fig. 7.

Are the densities obtained in Fig. 7 close to what could be expected for our systems? The complete phonon (or rotation) spectrum of the SAMs is very complex simply because the number of atoms per unit cell is large. However, as far as we are concerned with long-wavelength modes compared to a scale defined by the molecular interaction, we can, in principle, forget all the details of the motif and describe the equilibrium properties of the system with a continuum elastic theory. We assume in the following that the films we are considering could be described by such theory. In the two types of monolayer studied in this work the molecules are organized in a triangular lattice. Due to symmetry consideration, it is well known that such a lattice can be described by a unique pair of Lamé coefficients (λ, μ).[58] The displacement field is then a sum of two independent contributions, a longitudinal and a transverse components. The wave equation to be considered is[58]

$$\left(\Delta + \frac{\omega^2}{\nu^2}\right) u(\vec{r}) = 0, \tag{39}$$

where $u(\vec{r})$ is any component, longitudinal or transverse, of the displacement field and ν the corresponding sound veloc-

ity. Equation (39) may be considered as the simplest possible candidate to describe the mechanical properties of the SAMs. The density of states obtained with this model gives a reference to compare to the results of Fig. 7,

$$\rho(\omega) = \frac{1}{2\pi\nu^2}\omega. \tag{40}$$

With this simple continuum elastic theory, the density of harmonic modes at low frequencies is linear and characterized solely by the speed of sound. Considering the linear density [Eq. (40)] suppresses dissipation. This is particularly clear with the Cole-Cole model [Eqs. (B4) and (38)]: taking $n=1$ gives $S_{Cole\text{-}Cole}(\omega)=0$. If our systems were perfectly ordered at the macroscopic scale probed in the frequency window considered in this work, the motion of the permanent dipoles would occur without any dissipation. Since we observe dissipation the density of states cannot be perfectly linear as in Eq. (40). Indeed, in the two examples shown in Fig. 7, clear deviations to the linear relation are evidenced.

Considering the model structure of the SAMs described in Sec. III, nonlinearities in the density of states are induced by disorder. There is several ways to introduce disorder in the continuum elastic theory. A direct generalization of Eq. (39) is investigated in Ref. 59. As a matter of illustration we base our following discussion on this particular example which has the merit to propose analytical expressions. Considering polycrystalline materials, such as our monolayers, and special type of disorder where λ is taken as the only random variable, the original continuum elastic theory is simplified to a wave equation for a displacement field that is reduced to a scalar instead of a two-component vector[59]

$$\left[\Delta + \frac{\omega^2}{\nu^2(\vec{r})}\right]u(\vec{r}) = 0. \tag{41}$$

$\nu(\vec{r})$ is the random sound velocity field. Correlated noise is considered by the authors of Ref. 59 with mean ν and spatial correlation $\langle\nu(\vec{r})\nu(\vec{r}')\rangle=\exp(-|\vec{r}-\vec{r}'|/l_c)$, l_c being the correlation length. Standard perturbation theory gives the density of states for $\omega \ll v/l_c$,[59]

$$\rho(\omega) = \frac{1}{2\pi\nu^2}\omega\left[1 + \alpha\left(\frac{l_c}{\nu}\right)^2\omega^2 + \cdots\right]. \tag{42}$$

α is a positive constant to be determined. We note in the above equation a nonlinear increase, $\delta\rho$, of the density of states

$$\delta\rho(\omega) = \alpha\frac{l_c^2}{2\pi\nu^4}\omega^3. \tag{43}$$

The nonlinear part of the density of states of harmonic modes is at the origin of the friction in the generalized Langevin equation. In other words, there is dissipation only because some sort of disorder exists in our systems. An example of such nonlinear contribution induced by disorder is given by Eq. (43). In this relation, the amplitude of $\delta\rho$ depends on l_c and ν. If the first parameter is certainly related to the particular model used in Ref. 59, the second one is much more general. If one omits the Poisson ratio, the average speed of sound is expressed as $\nu \propto \sqrt{E/\rho_M}$, where E is the Young's modulus and ρ_M the mass density of the SAM.[58] The Young's modulus expresses the property of a body to be elongated (or compressed) by a uniform extension (or compression) along the direction where the stress is applied. Equations such as Eqs. (37) and (43) build therefore a natural connection between the dynamic of relaxation of the permanent dipoles and the mechanical properties of the molecular junctions, a key parameter that controls these properties being the Young's modulus. As it was pointed out in the introduction of Ref. 21, it seems suitable to complement the admittance spectroscopy by investigations of the mechanical properties of the self-assembled monolayers. A few questions related to the present work could concern the comparison of the speed of sound in OTS- and OD-based junctions or the effects of a perpendicular dc electric field on the Young's modulus. Note that the Young's modulus was very recently measured for similar SAMs as ours and shown to be close to the one of bulk polyethylene, giving a speed of sound $\nu = 2000$ m s^{-1}.[60] The parameters of the dielectric susceptibility $(n, m, 1/\tau)$ found for our systems are also close to the ones of bulk saturated polymers.

VIII. CONCLUSIONS

In this work we focus on the dipolar component of the complex admittance.[23] It is attributed to permanent dipoles present in the monolayer. The measured response is a system average which contains elements both from the dipoles and from the mechanical interaction of these dipoles with the electrically inactive structure of which the dipoles are an intrinsic part. This has been modeled in terms of the GLE that considers a permanent dipole trapped in a harmonic potential and interacting with a non-Markovian bath.[26] This equation allows us to connect the spectral density of polarization noise to the measured dielectric susceptibility. From our experimental data we have determined the power spectrum of this noise: it is of $1/f$ type. It is of importance since all fluctuating mechanisms existing in our systems ($1/f$ current noise, random telegraph signal, etc.) should be considered by taking into account explicitly this high-level noise. We suggest, for instance, that the polarization noise could be the source of the $1/f$ current noise observed earlier in the same systems.[15] Finally, we stress that in order to get more physical insight into the mechanisms at the origin of the particular complex admittance investigated in this work, studies of the mechanical properties of the molecular junctions should be carried on.

APPENDIX A: SPECTRAL DENSITY OF THE RANDOM FIELD

In this appendix, we derive a relation between the local susceptibility, χ, and the spectral density of the random field, ξ. From Eq. (19) we write

$$\tilde{\eta}(s) = \frac{1}{s}\left[\frac{1}{\chi(js)} - \frac{1}{\chi_0}\right]. \tag{A1}$$

According to Eq. (14), the memory function and the spectral density are related by an integral relation. Inverting this relation gives[28]

$$\gamma(\omega) = \lim_{\epsilon \to 0^+} [\tilde{\eta}(\epsilon + j\omega) + \tilde{\eta}(\epsilon - j\omega)]. \quad \text{(A2)}$$

Using these two equations we can determine the spectral density of the environmental coupling from the dielectric susceptibility

$$\gamma(\omega) = \frac{\Im\chi(\omega)}{|\chi(\omega)|^2}. \quad \text{(A3)}$$

Inserting the last expression into Eq. (14) we get a relation between the friction kernel and the local susceptibility ($\beta = 1/k_B T$),

$$\eta(t) = \beta\langle\xi(t)\xi(0)\rangle = \int_0^{+\infty} d\omega \frac{\Im\chi(\omega)}{\omega|\chi(\omega)|^2}\cos\,\omega t. \quad \text{(A4)}$$

By virtue of Wiener-Khintchine's theorem the spectral density of the random field is deduced

$$S(\omega) = 4k_B T \frac{\Im\chi(\omega)}{\omega|\chi(\omega)|^2}. \quad \text{(A5)}$$

APPENDIX B: MODEL SPECTRAL DENSITIES OF NOISE

In this appendix, we derive from Eq. (24) the noise spectral density corresponding to dielectric model susceptibilities: the Debye,[44] Cole-Cole,[45] and Cole-Davidson[46] susceptibilities.

The Debye susceptibility,

$$\chi_{Debye}(\omega) = \frac{\chi_0}{1 + j\omega\tau} \quad \text{(B1)}$$

gives a white noise

$$S_{Debye}(\omega) = \frac{4k_B T}{\chi_0}. \quad \text{(B2)}$$

This is typical of usual Brownian motion where, in the free-particle case (without trapping potential), the system experiences a normal diffusion under the action of a memoryless damping function, $\eta_{Debye}(t) = \eta_S \delta(t)$.[54] This type of motion is characterized, for instance, by a mean-square displacement linear in time. Note that this simple case is also of direct interest for us since the low-frequency peak is Debye type (see Fig. 1).[23]

The Cole-Cole susceptibility[45]

$$\chi_{Cole\text{-}Cole}(\omega) = \frac{\chi_0}{1 + (j\omega\tau)^{1-n}} \quad \text{(B3)}$$

yields a completely different result

$$S_{Cole\text{-}Cole}(\omega) = \frac{4k_B T}{\chi_0}\tau(\omega\tau)^{-n}\sin(1-n)\frac{\pi}{2}. \quad \text{(B4)}$$

$S_{Cole\text{-}Cole}$ decreases following the same power law in the whole frequency range. This is the signature of a fractional Gaussian noise with Hurst index $H = (n+1)/2$.[29,30] In the free-particle case, this is typical of a strict subdiffusion with a non-Markovian damping kernel $\eta(t) \propto t^{n-1}$. This type of dynamics is characterized, for instance, by a mean-square displacement increasing in time as a power law with an exponent less than 1.

Last, the Cole-Davidson susceptibility[46]

$$\chi_{Cole\text{-}Davidson}(\omega) = \chi_0(1 + j\omega\tau)^{n-1} \quad \text{(B5)}$$

shows two distinct regimes

$$S_{Cole\text{-}Davidson}(\omega) = \frac{4k_B T}{\chi_0}\frac{\sin(1-n)\omega\tau}{\omega}(1 + \omega^2\tau^2)^{(1-n)/2}. \quad \text{(B6)}$$

It gives a plateau at small frequencies ($\omega\tau \ll 1$) and a power law, ω^{-n}, at high frequencies ($\omega\tau \gg 1$).

The Debye and Cole-Cole models are both well studied. They serve here as references illustrating two different types of dynamics to compare with. The Cole-Davidson model in a sense is an extrapolation between these two different cases: it shows a Debye character at low frequencies and a Cole-Cole character at high frequencies.

[1] F. Schreiber, Prog. Surf. Sci. **65**, 151 (2000).
[2] J. Collet, O. Tharaud, A. Chapoton, and D. Vuillaume, Appl. Phys. Lett. **76**, 1941 (2000).
[3] M. Halik, H. Klauk, U. Zschieschang, G. Schmid, C. Dehm, M. Schütz, S. Maisch, F. Effenberger, M. Brunnbauer, and F. Stellacci, Nature (London) **431**, 963 (2004).
[4] A. Facchetti, M. H. Yoon, and T. K. Marks, Adv. Mater. **17**, 1705 (2005).
[5] E. Stern, J. F. Klemic, D. A. Routenberg, P. N. Wyrembak, D. B. Turner-Evans, A. D. Hamilton, D. A. LaVan, T. M. Fahmy, and M. A. Reed, Nature (London) **445**, 519 (2007).
[6] Z. Liu, A. A. Yasseri, J. S. Lindsey, and D. F. Bocian, Science **302**, 1543 (2003).
[7] V. Ferri, M. Elbing, G. Pace, M. D. Dickey, M. Zharnikov, P. Samori, M. Mayor, and M. A. Rampi, Angew. Chem., Int. Ed. Engl. **47**, 3407 (2008).
[8] C. Dri, M. Peters, J. Schwarz, S. Hecht, and L. Grill, Nat. Nanotechnol. **3**, 649 (2008).
[9] N. Katsonis, T. Kudernac, M. Walko, S. Van der Molen, B. Van Wees, and B. Feringa, Adv. Mater. **18**, 1397 (2006).
[10] J. M. Mativetsky, G. Pace, M. Elbing, M. A. Rampi, M. Mayor, and P. Samori, J. Am. Chem. Soc. **130**, 9192 (2008).
[11] A. Salomon, D. Cahen, S. M. Lindsay, J. Tomfohr, V. B. Engelkes, and C. D. Frisbie, Adv. Mater. **15**, 1881 (2003).
[12] H. Haick and D. Cahen, Prog. Surf. Sci. **83**, 217 (2008).
[13] W. Wang, T. Lee, T. Krestchmar, and M. A. Reed, Nano Lett. **4**, 643 (2004).
[14] A. Troisi, J. M. Beebe, L. B. Picraux, R. D. van Zee, D. R. Stewart, M. A. Ratner, and J. G. Kushmerick, Proc. Natl. Acad. Sci. U.S.A. **104**, 14255 (2007).

[15] N. Clément, S. Pleutin, O. Seitz, S. Lenfant, and D. Vuillaume, Phys. Rev. B **76**, 205407 (2007).
[16] A. Badia, R. B. Lennox, and L. Reven, Acc. Chem. Res. **33**, 475 (2000).
[17] V. V. Tsukruk, Adv. Mater. **13**, 95 (2001).
[18] A. Haran, D. H. Waldeck, R. Naaman, E. Moons, and D. Cahen, Science **263**, 948 (1994).
[19] M. Pursch, D. L. Vanderhart, L. C. Sander, X. Gu, T. Nguyen, S. A. Wise, and D. A. Gajewski, J. Am. Chem. Soc. **122**, 6997 (2000).
[20] H. Schmitt, A. Badia, L. Dickson, L. Reven, and R. B. Lennox, Adv. Mater. **10**, 475 (1998).
[21] Q. Zhang, Q. Zhang, and L. A. Archer, J. Phys. Chem. B **110**, 4924 (2006).
[22] M. C. Scott, D. R. Stevens, J. R. Bochinski, and L. I. Clarke, ACS Nano **2**, 2392 (2008).
[23] N. Clément, S. Pleutin, D. Guérin, and D. Vuillaume, Phys. Rev. B **82**, 035404 (2010).
[24] A. K. Jonscher, Nature (London) **267**, 673 (1977).
[25] A. O. Caldeira and A. J. Leggett, Ann. Phys. **149**, 374 (1983).
[26] I. Goychuk, Phys. Rev. E **76**, 040102(R) (2007).
[27] P. C. E. Stamp, Stud. Hist. Philos. Mod. Phys. **37**, 467 (2006).
[28] U. Weiss, *Quantum Dissipative Systems*, 3rd ed. (World Scientific, Singapore, 2008).
[29] B. B. Mandelbrot and J. W. Van Ness, SIAM Rev. **10**, 422 (1968).
[30] S. C. Kou and X. S. Xie, Phys. Rev. Lett. **93**, 180603 (2004).
[31] D. K. Aswal, S. Lenfant, D. Guerin, J. V. Yakhmi, and D. Vuillaume, Anal. Chim. Acta **568**, 84 (2006).
[32] A. Salomon, T. Boecking, C. K. Chan, F. Amy, O. Girshevitz, D. Cahen, and A. Kahn, Phys. Rev. Lett. **95**, 266807 (2005).
[33] E. H. Nicollian and J. R. Brews, *MOS (Metal Oxide Semiconductor) Physics and Technology* (Wiley, New York, 1982).
[34] Y. Wang, Rev. Sci. Instrum. **74**, 4212 (2003).
[35] G. G. Raju, *Dielectrics in Electric Fields* (Marcel Dekker, New York, Basel, 2003).
[36] M. R. Linford, P. Fenter, P. M. Eisenberger, and C. E. D. Chidsey, J. Am. Chem. Soc. **117**, 3145 (1995).
[37] K. I. Iimura, Y. Nakajima, and T. Kato, Thin Solid Films **379**, 230 (2000); I. Doudevski and D. K. Schwartz, J. Am. Chem. Soc. **123**, 6867 (2001).
[38] I. M. Tidswell, B. M. Ocko, P. S. Pershan, S. R. Wasserman, G. M. Whitesides, and J. D. Axe, Phys. Rev. B **41**, 1111 (1990).
[39] I. M. Tidswell, T. A. Rabedeau, P. S. Pershan, S. D. Kosowsky, J. P. Folkers, and G. M. Whitesides, J. Chem. Phys. **95**, 2854 (1991).
[40] L. Romaner, G. Heimel, C. Ambrosch-Draxl, and E. Zojer, Adv. Funct. Mater. **18**, 3999 (2008).
[41] R. Kubo, J. Phys. Soc. Jpn. **12**, 570 (1957).
[42] L. F. Cugliandolo, J. Kurchan, and G. Parisi, J. Phys. I **4**, 1641 (1994).
[43] N. Pottier, Physica A **317**, 371 (2003).
[44] P. Debye, *Polar Molecules* (Dover, New York, 1965).
[45] K. S. Cole and R. H. Cole, J. Chem. Phys. **9**, 341 (1941).
[46] D. W. Davidson and R. H. Cole, J. Chem. Phys. **19**, 1484 (1951).
[47] S. Havriliak and S. Negami, Polymer **8**, 161 (1967).
[48] L. A. Dissado and R. M. Hill, Nature (London) **279**, 685 (1979); Proc. R. Soc. London **390**, 131 (1983).
[49] L. J. Slater, *Generalized Hypergeometric Functions* (Cambridge University Press, Cambridge, England, 2008).
[50] R. M. Hill, Phys. Status Solidi B **103**, 319 (1981).
[51] S. Corezzi, E. Campani, P. A. Rolla, S. Capaccioli, and D. Fioretto, J. Chem. Phys. **111**, 9343 (1999).
[52] N. V. Prokof'ev and P. C. E. Stamp, Rep. Prog. Phys. **63**, 669 (2000).
[53] A. O. Caldeira, A. H. Castro Neto, and T. O. de Carvalho, Phys. Rev. B **48**, 13974 (1993).
[54] S. Chandrasekhar, Rev. Mod. Phys. **15**, 1 (1943).
[55] K. S. Ralls, W. J. Skocpol, L. D. Jackel, R. E. Howard, L. A. Fetter, R. W. Epworth, and D. M. Tennant, Phys. Rev. Lett. **52**, 228 (1984).
[56] S. M. Kogan, *Electronic Noise and Fluctuations in Solids* (Cambridge University Press, Cambridge, 1996).
[57] N. E. Israeloff, Phys. Rev. B **53**, R11913 (1996).
[58] L. D. Landau and E. M. Lifshitz, *Theory of Elasticity* (Pergamon, New York, 1970).
[59] V. Gurarie and A. Altland, Phys. Rev. Lett. **94**, 245502 (2005).
[60] F. W. DelRio, C. Jaye, D. A. Fischer, and R. F. Cook, Appl. Phys. Lett. **94**, 131909 (2009).